

Initial quality performance results using a phantom to simulate chest computed radiography

Wilbroad Muhogora, Renato Padovani¹, Peter Msaki

Department of Physics, University of Dar es Salaam, P.O Box 35063, Dar es Salaam, Tanzania. ¹Fisica Sanitaria, Ospedale Universitario, P.le Santa Maria della Misericordia 15, 33100, Udine, Italy

Received on: 07.05.10

Review completed on: 03.06.10

Accepted on: 30.07.10

ABSTRACT

The aim of this study was to develop a homemade phantom for quantitative quality control in chest computed radiography (CR). The phantom was constructed from copper, aluminium, and polymethylmethacrylate (PMMA) plates as well as Styrofoam materials. Depending on combinations, the literature suggests that these materials can simulate the attenuation and scattering characteristics of lung, heart, and mediastinum. The lung, heart, and mediastinum regions were simulated by 10 mm x 10 mm x 0.5 mm, 10 mm x 10 mm x 0.5 mm and 10 mm x 10 mm x 1 mm copper plates, respectively. A test object of 100 mm x 100 mm and 0.2 mm thick copper was positioned to each region for CNR measurements. The phantom was exposed to x-rays generated by different tube potentials that covered settings in clinical use: 110-120 kVp (HVL=4.26-4.66 mm Al) at a source image distance (SID) of 180 cm. An approach similar to the recommended method in digital mammography was applied to determine the CNR values of phantom images produced by a Kodak CR 850A system with post-processing turned off. Subjective contrast-detail studies were also carried out by using images of Leeds TOR CDR test object acquired under similar exposure conditions as during CNR measurements. For clinical kVp conditions relevant to chest radiography, the CNR was highest over 90-100 kVp range. The CNR data correlated with the results of contrast detail observations. The values of clinical tube potentials at which CNR is the highest are regarded to be optimal kVp settings. The simplicity in phantom construction can offer easy implementation of related quality control program.

Key words: Computed radiography, contrast-to-noise ratio, image quality, quality control phantom

Introduction

Recent years have witnessed many radiology departments in developed countries switching from screen-film to digital systems. Similar wave of change is now sweeping across developing countries such as in Tanzania where there are currently three operational computed radiography (CR) systems with existing plans to establish such units in several government hospitals. CR technology is considered as a


cost-effective route to digital imaging since the existing x-ray equipment can be utilized and the work flow pattern is not affected significantly.^[1] The chief advantages of CR systems include the capability to optimize the image quality through post image processing techniques, the ability to store or transmit the images electronically and re-usability of the detector.^[2,3] Other advantages are the inherent wide dynamic range, which can reduce the repeat rate and low running costs because wet chemistry film processing method is not applied.^[2,3] However, in order to fully utilize these benefits, it is necessary to evaluate the actual capabilities of the CR systems through acceptance testing and implementation of regular quality control (QC) programs^[3] The latter requirement is necessitated by the fact that CR systems have complex image acquisition and processing schemes that can easily lead to unnoticed image quality degradation.^[2-4]

Phantoms are usually employed during implementation of QC measurements with an overall aim to notice any changes in the imaging system. The phantom should be able to reproduce as closely as possible the changes of x-ray energy after passing through structures of standard sized patients. Presently, this requirement is difficult to

Address for correspondence:

Mr. Wilbroad E. Muhogora
Department of Physics, University of Dar es Salaam,
P. O. Box 35063 Dar es Salaam, Tanzania.
E-mail:wmuhogora@yahoo.com

Access this article online

Quick Response Code: 	Website: www.jmp.org.in
	DOI: 10.4103/0971-6203.75468

be fulfilled by any single phantom.^[4] There are different types of phantoms currently available on market,^[5,6] and many of them utilize subjective evaluations. One of the disadvantages of subjective evaluations is the inter-observer variations, which tend to reduce the reliability of the results. The reliability can be improved if quantitative or semi-quantitative methods are applied in performing QC tests. However, currently there are few simple methods that can promote regular undertaking of such tests. The objective of this study was to construct a simple homemade phantom that applies the recommended concept of CNR in digital mammography for routine QC test in chest CR.

Materials and Methods

Phantom construction

The basic design of this phantom was adapted from the digital chest radiography phantom (Nuclear Associates Model 07-646, Nuclear Associates, Carl Place, NY) described elsewhere.^[7,8] The Nuclear Associates phantom was modified in terms of material composition, layout, and incorporated test objects for CNR measurements. The modified phantom consists of copper (Cu), aluminum (Al), polymethylmethacrylate (PMMA), and styrofoam (polystyrene) materials. These materials have been found to be suitable to simulate the X-ray attenuation and scatter properties similar to those of chest and sub-diaphragm regions.^[7,9,10] In diagnostic energy range, the contrast between soft tissue and bone is enhanced by photoelectric interactions, which vary approximately with the cube of the

atomic number (Z) of the element or effective Z (Z_{eff}) of the object. This implies that Al ($Z=13$) would make the photoelectric interactions to be similar interactions in soft tissue ($Z_{\text{eff}} = 7.2$) and bone ($Z_{\text{eff}}=13.8$) that can be found in clinical practice. Although Cu ($Z=29$) tends to reduce photoelectric interactions due its effect of shifting of exit spectrum to higher energy side, its inclusion in the phantom was adopted from literature information.^[7,9,10] Like in many other geometric phantoms, this remains to be a major weakness of the developed phantom [Figure 1].

The layout of the phantom, which is shown in Figure 1, consists of six layers described from bottom to top as follows: the first layer (bottom most) is made up of 300 mm × 300 mm × 20 mm PMMA followed by 300 mm × 300 mm × 10 mm Al sheet as the second layer. The second layer of Al sheet holds four Cu plates positioned as follows: a circular 0.5 mm thick Cu plate of 105 mm diameter at the center to simulate the heart; two Cu plates each of 100 mm × 100 mm and 0.25 mm thickness (i.e. 0.5 mm Cu total thickness) at two corners above the heart to simulate the lung region and a Cu strip of 124 mm x 30 mm and 1 mm thickness below the heart to simulate subdiaphragm regions. As stated before, the thicknesses of PMMA, Al, and Cu plates or strips were adopted from a Nuclear Associates Model 07-646 phantom.^[7,8] Between lungs, a 5 lp mm⁻¹ resolution test pattern, type 07-553 (Nuclear Associates, Carla Place, New York) incorporating 0.05 mm Pb was positioned at 45° to the horizontal plane for limiting resolution measurements. The constructed phantom for

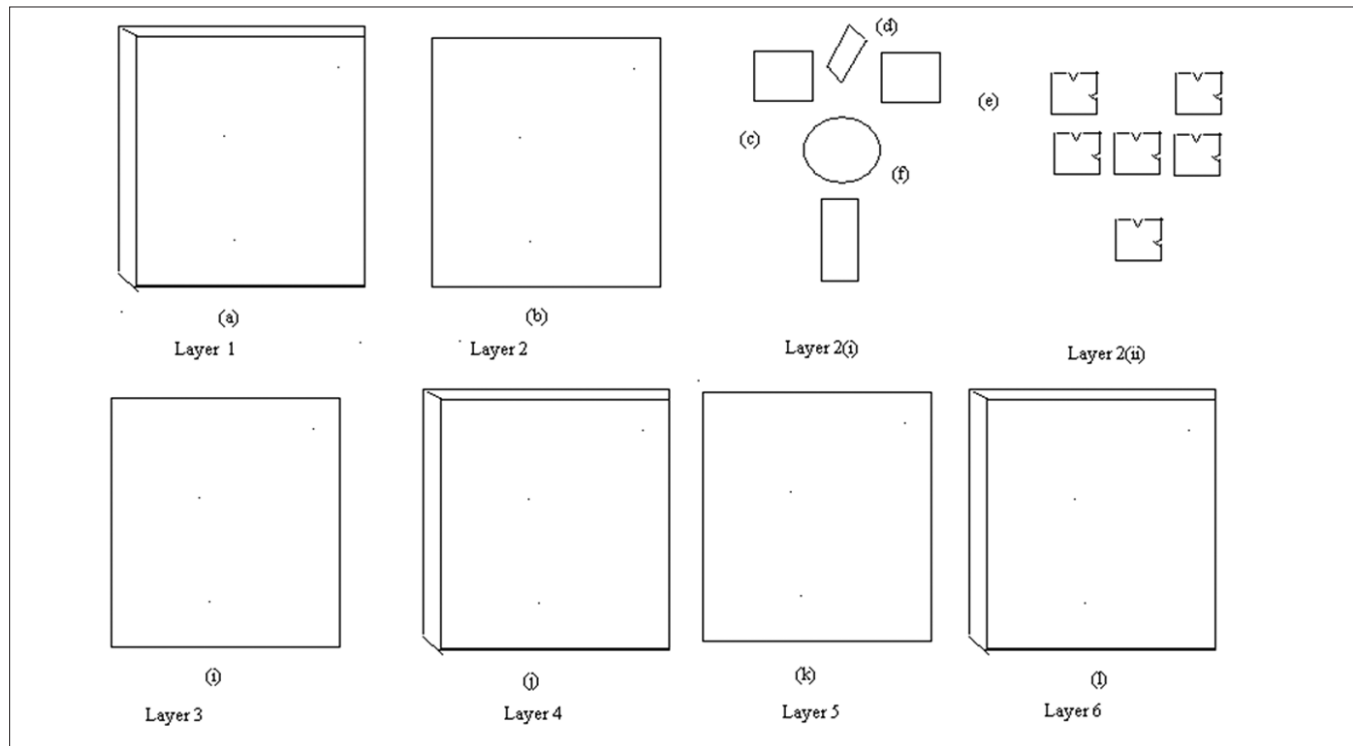


Figure 1: Schematic lay out of constructed phantom. Layer 1 form the bottom most part of phantom while layer 6 is its uppermost part

CNR measurements do not incorporate resolution,^[11] which would be complemented by the measurements by the incorporated resolution test pattern. The resolution test pattern can also be useful to identify the phantom orientation. On top of each lung, heart, and subdiaphragm regions, a 0.1 mm thick Cu test object (plate) of 100 mm x 100 mm dimensions was positioned at center for CNR measurements. The lungs had a total of four such test objects; each of two objects placed on a 0.1 mm Cu plate and each of the other two objects placed directly on Al (layer 2). The use of a pair of Cu test object for each lung was intended to investigate the level of contrast achieved by 0.1 mm Cu test object placed on a 0.1 mm Cu plate in comparison to the contrast if such test object is placed on Al. Although a Cu plate is often used in similar phantoms, the authors had a view that the simulated interactions by the Cu plate may not be comparable to interactions in the lung because of very large difference between their atomic numbers. The selection of 0.1 mm thick copper as a test object for CNR measurements was based on typical thickness of details of interest in chest radiography. In similar studies, copper test objects with thickness ranging 0.006-0.0076, 0.013-0.127 and 0.051-0.406 mm were used to simulate lung, heart, and mediastinum, respectively.^[7,12-15] Therefore a copper test object of 0.1 mm thickness was considered to be a representative of contrast important to clinical imaging of chest. The third layer was made up of 300 mm x 300 mm x 50 mm styrofoam slab, to simulate air gap in the thoracic cavity. The fourth layer was made up of 300 mm x 300 mm x 20 mm PMMA followed by the fifth layer of 300 mm x 300 mm x 10 mm Al. The sixth layer (upper most part) was completed by 300 mm x 300 mm x 20 mm PMMA. The phantom parts were tied together by a tape. The dimensions of assembled phantom are 300 mm x 300 mm x 146 mm and weighs 7.3 kg.

Besides the layout and sequence of construction materials, the difference between the phantom in this study and that designed by the Nuclear Associates is the provision of regions of interest (ROIs) on copper plates on the earlier phantom for CNR measurements. Instead of ROIs for CNR measurements, the Nuclear Associates phantom has copper disks of varying thicknesses for contrast-detail studies and also has provisions of the anatomic components for optical density measurements. Despite these differences, the phantom is similar to previously studied phantoms in terms of construction materials and some of the thicknesses of these materials.^[7-9,12-15] The constructed phantom was used to determine CNR measurements of its images acquired on imaging system described in the next section. A single 35 cm x 43 cm general plate (GP) was used for all measurements so that uniform plate sensitivity is ensured for reproducible measurements.

Equipment

Tests were performed with a general purpose Philips

Optimus Bucky Diagnost (Phillips Medical Systems, Hamburg, Germany) with antiscatter grid (grid ratio, 12:1, 36 lp cm⁻¹) focused at 130 cm towards the wall stand. The employed CR reader was the newly acquired Kodak Direct View CR 850A reader (Eastman Kodak Company, Rochester, New York) with Kodak GP plates (Carestream Health TH, Inc., Rochester, New York). The selection of this CR reader was based on the fact that only CR images from this unit could be copied to the flash disk for transferring to a desktop computer and workstation for CNR measurements and contrast-details observations, respectively. Prior to this study, the x-ray equipment had been tested for constancy and its performance found adequate. In particular, the kVp accuracy and output reproducibility for 70-120 kVp range were within $\pm 5\%$ and $\pm 1\%$, respectively. In the same kVp range, the half value layer (HVL) measurements varied from 2.77 to 4.66 mm Al. The phantom was exposed in terms of entrance air kerma (EAK) as measured by using a calibrated ionization chamber Radcal (model 20X6-60 with electrometer model 2026C) (Radcal Corporation, Monrovia, California) The following tests were all performed at 180 cm SID towards the wall stand on antiscatter grid.

Reproducibility test

The purpose of reproducibility test was to verify if repeated radiographic exposures on the phantom give consistent CNR results under exposure conditions similar to wall stand chest x-ray examinations. During this test, the grid was used in consistency to local clinical practice. A constant EAK of 300 μ Gy (achieved by mAs changing), which was selected on the basis of typical diagnostic reference level (DRL), was used in all phantom exposures. It is known that DRL usually varies between 200 to 400 μ Gy for chest x-ray examinations.^[16] The phantom was exposed at 110 kVp with a constant EAK of 300 μ Gy ($\pm 5\%$) at 180 cm source to image distance (SID). The exposed image plate was read out on Kodak CR 850A scanner with all post-processing algorithms turned off. This process was repeated nine more times. For each phantom CR image, CNR was determined for the lung, heart, and mediastinum ROIs as described in section of CNR evaluation and contrast detail analysis.

Influence of tube potential on phantom response

Appropriate selection of tube potential (kVp) during x-ray examination is crucial since it affects the radiographic contrast of the resulting image under constant detector conditions. Therefore the purpose of this study was to investigate the dependence of CNR on tube potential at constant EAK to the phantom for the wall stand technique. At the hospital where this study was undertaken, the kVp in use for the wall stand technique vary from 110 to 120 kVp at 180 cm SID. During this study, the kVp ranging from 70 to 120 kVp were selected so that clinical tube potentials are also included. Consequently they ranged from 70 to 120 kVp for the wall stand technique. For each kVp setting, the image was acquired by exposing the phantom with a

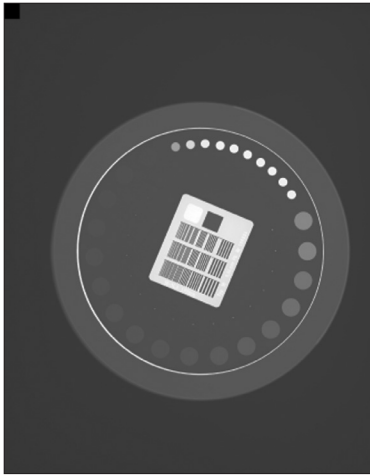


Figure 2: The CR image of Leeds TOR CDR test object with visible 11 mm diameter size details and 5.6 mm diameter size disks

constant EAK of $300 \mu\text{Gy} (\pm 5\%)$ achieved by mAs changing and read out by Kodak CR 850A unit with post-processing algorithms turned off.

Subjective image quality evaluation

The purpose of this study was to investigate if the kVp dependence of CNR correlated with that of details visibilities for the constructed phantom. For this purposes, a Leeds TOR CDR test object (University of Leeds, Leeds, UK) [Figure 2] was used for contrast-detail analysis. This test object is designed for QC in screen film radiography as well in digital radiography. It consists of four test patterns as follows: a limiting resolution test pattern (up to $14.3 \text{ cycles mm}^{-1}$), which acts as useful measure of unsharpness, calibrated grey scale that consists of 10 disks each of 5.6 mm diameter arranged along an arc for film base/fog level, relative and contrast measurements; an array of 17 disks low contrast details each of 11 mm diameter and an array of 17 disks high contrast details each of 0.5 mm diameter. The test with low contrast details is sensitive to noise and film gamma where applicable while that with high contrast objects is sensitive to noise and film gamma as well as unsharpness^[17] [Figure 2].

For this purpose, the TOR CDR test object was positioned at the second layer (on aluminium sheet) of the constructed phantom in order to simulate similar scattering conditions to Leeds TOR CDR object as during acquisition of images for CNR measurements. During this test, the copper plates and copper test objects were removed. The images of TOR CDR test object were then acquired under the same conditions as during CNR measurements i.e. same exposure parameters, geometry, constant EAK of $300 \mu\text{Gy} (\pm 5\%)$, and post-processing turned off.

CNR evaluation and contrast detail analysis

The acquired radiographic images of the phantom were copied to a flash disk and transferred to desk top computer for analysis using the image processing and analysis

freeware software, *image J* in (<http://rsb.info.nih.gov/ij/>).^[18,19] Mean pixel values and pixels standard deviation values were measured and used to calculate the contrast-to-noise ratio (CNR) values according to equation (1):^[20,21]

$$CNR = \frac{PV_b - PV_{Cu}}{\sqrt{[1/2(\sigma_b^2 + \sigma_{Cu}^2)]}}, \quad \dots\dots(1)$$

where PV_b is the mean pixel value in the neighboring background of copper (Cu) test object, PV_{Cu} is the mean pixel value in the center of 0.1 mm thick Cu test object, σ_b^2 is the standard deviation of pixel values in the neighboring background of Cu and σ_{Cu}^2 is the standard deviation in the center of 0.1 mm thick Cu test object.

The images of Leeds TOR CDR were transferred to a dedicated display monitor type BARCO MED (BARCO VIEW, Belgium), which is used for presentation for contrast detail scoring. Three people (two physicists and one technologist) experienced with the scoring process scored the Leeds TOR CDR images under subdued light conditions. During viewing of images, no restrictions on viewing time and viewing distance were imposed in order to mimic the clinical conditions. However, a detail was considered visible if its full size was completely visualized. In this way the subjectivity inherent in the scoring process could be reduced. Starting from the highest contrast, the number of details seen was counted and recorded by each observer. The overall score was determined as the average score of the number of details seen from three sets of observations. The scoring variation among the observers was determined as the standard deviation of individual scores.

Results and discussion

Phantom reproducibility

The short-term reproducibility of the constructed phantom is presented in Figure 3. The ratio of the maximum to minimum (max/min) exposure index (EI) was 1.02 and hence good stability. The EI is an indicator of detector dose for Kodak CR systems^[3] [Figure 3].

Influence of tube potential on CNR

The variation of CNR with kVp is presented in Figure 4. The detailed information during image acquisition is shown in Table 1. The CNR values decreased with increasing beam quality as expected since CNR falls with beam quality.^[1,22] CNR is known to depend on absorption characteristics of the detector, pixel size, radiation spectrum, detector dose, and the object in beam.^[23] Considering these influencing factors, it is clear that the radiation spectrum and hence detector dose were the only varying factors and therefore sole determinants of CNR. The highest CNR values were observed at 70 kVp while the lowest CNR were observed at

120 kVp for all test objects [Figure 4]. Considering possible clinical kVp range for such technique, 90 kVp appears to be the setting that would results to the highest CNR. Table 1 shows that EI increased with kVp due to increasing dose to the detector as expected^[24] while the resolution remained almost constant. Two observers each scored 2.9 lp mm⁻¹ at 90 kVp while the third observer scored 3.5 lp mm⁻¹ resulting to lower average value in comparison to the resolutions at other tube potentials. The reason for this observation is not precisely known. However, the resolution is influenced by the detector-related factors (effective aperture size, spatial sampling interval between measurements or lateral signal spreading effects) as well as to other geometrical factors (effective size of the x-ray source, object and image receptor during exposure).^[25] The observed resolution constancy implies that these factors were practically constant during the acquisition of images [Table 1].

Contrast detail analysis

The results of subjective image quality evaluation are presented in Figure 5. Table 2 provides information during image acquisition for a wall stand technique. As shown in Figure 5, the detail visibility varied with kVp and was relatively higher at low beam qualities. As already known, the photoelectric effect tends to enhance contrast at low photon energies.^[22] The inter observer variations are indicated by error bars expressed as the standard deviation of the three scores. For both techniques, the visibility of 0.5 mm size details (high contrast) was higher than that of 11 mm size details (low contrast). The low visibility has been attributed to the influence of system noise, which is known to affect the low contrast objects.^[25] The number of visible details for all sizes was highest at low beam quality and the lowest at highest beam quality for a wall stand technique [Figure 4]. Therefore there is a correlation between the contrast detail results and the CNR data [Figure 5] [Table 2].

It is increasingly recognized that screen-film-based techniques on chest x-ray examinations may not be suitable for digital radiography systems because the sensitivity of the atomic number of dominant elements present in digital detectors (Ba, CsI, or Se) declines at higher beam quality.^[3,11,12,15,26-28] The results of this study suggest similar views. Traditionally, a high kV technique (≥ 100 kVp) in screen-film-based chest x-ray examinations was intended to provide better penetration of the mediastinum and reduce the visibility of ribs to enable conspicuity of soft structures in lungs.^[29] In clinical digital imaging, the earlier reason is of less importance because of higher dynamic range of digital detectors. In practice, both high and low kVp techniques are in use depending on the clinical task as directed by the radiologist. Therefore the constructed phantom can be of use for high and low kVp chest CR.

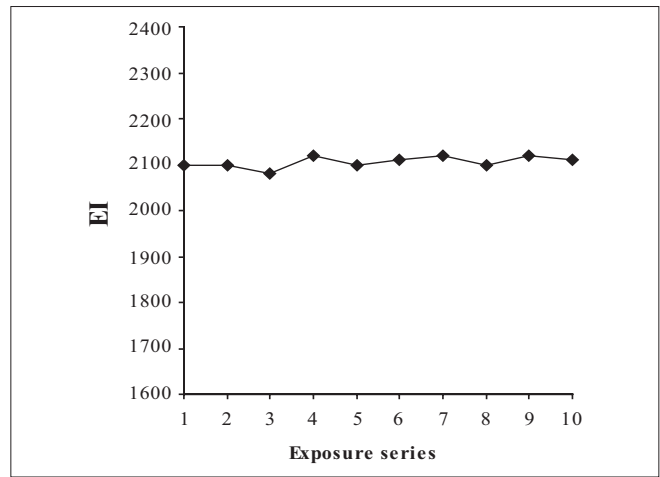


Figure 3: Short-term reproducibility of phantom exposed at 110 kVp (Half value layer= 4.26) (wall stand, source-image distance=180 cm)

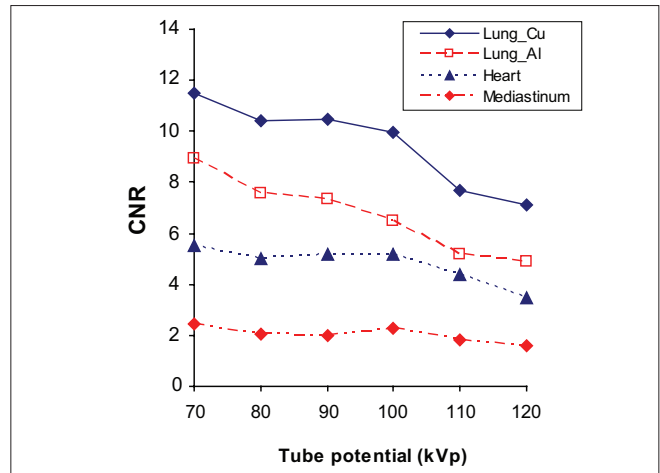


Figure 4: Variation of CNR with tube potential for the wall stand technique (source-image distance=180 cm) with antiscatter grid used

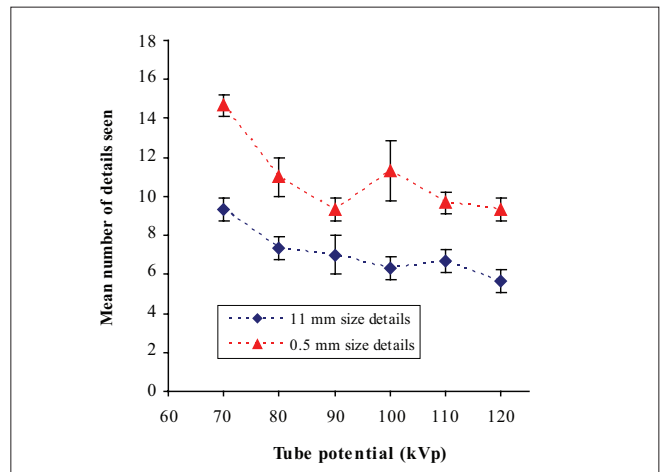


Figure 5: Number of details seen as a function of tube potential for the wall stand technique (source-image distance=180 cm) with antiscatter grid used. Low contrast details are shown as 11 mm diameter size while high contrast details are shown as 0.5 mm diameter size

Table 1: Parameters for image acquisition of the constructed phantom for the wall stand technique (SID= 180 cm, focus to a phantom distance=160.9 cm, field size =350 x 350 mm)

Tube potential (kVp)	HVL (mm Al)	Tube charge (mAs)	Entrance air kerma (μGy)	Exposure index (EI)	Resolution (lpmm ⁻¹)
70	2.77	17	302.3	1840	3.5
80	3.12	12.5	290	1930	3.5
90	3.53	10.6	307.8	2020	3.1
100	3.97	8.5	300.1	2050	3.5
110	4.26	7.1	296.7	2100	3.5
120	4.66	6.3	305.9	2100	3.5

Table 2: Parameters for image acquisition of the constructed phantom for wall stand technique (SID= 180 cm, focus to a phantom distance=160 cm, field size =350 x350 mm)

Tube potential (kVp)	HVL (mm Al)	Tube charge (mAs)	Entrance air kerma (μGy)	Exposure index (EI)
70	2.77	16	291.3	2030
80	3.12	12.5	290	1940
90	3.53	10	297.3	1820
100	3.97	8	289.2	2040
110	4.26	7.1	296.7	2100
120	4.66	6	298.3	2080

Conclusions

The usefulness of the constructed phantom in quality performance has been demonstrated. In this study, the maximum CNR was achieved at 90 kVp for clinically relevant chest wall conditions and this feature can be utilized for constancy tests in chest CR. Despite the fact that the phantom has been tested on a Kodak CR system, similar results are expected on other types of CR systems provided that they are functioning in accordance to acceptable performance standards. The use of different x-ray beam qualities is also unlikely to change the CNR trend. However, the limitation of the presented phantom like many other geometric phantoms is the use of copper and aluminium materials that can result into photoelectric interactions that are different from those provided by soft tissues and bones.

Acknowledgements

The work was supported by joint program of the International Centre for Theoretical Physics and the International Atomic Energy Agency (421.IAEA.02G) as well as the project on Safety and Efficacies for New Technology and Imaging using New equipment to Support European Legislation (SENTINEL FP-012909). The permission granted by the authority of the University Hospital (Udine) to undertake this study using hospital facilities is specially acknowledged. The technical assistance of M. Florean and E. Cragnolini on computed radiography facility is also appreciated

References

1. Vano EM, Faulkner K. A major advantage of digital imaging for

- general radiography is the potential for reduced patient dose so the film/screen systems should be phased out as unnecessary hazardous. *Med Phys* 2006;33:1529-31.
- Rowlands JA. The physics of computed radiography. *Phys Med Biol* 2002;47:R123-66.
 - American Association of Physicists in Medicine. Acceptance testing and quality control of photostimulable storage phosphor imaging systems. Report of AAPM Task Group 10; AAPM;2006.
 - Walsh C, Gorman D, Byrne P, Larkin A, Dowling A, Malone JF. Quality assurance of computed and digital radiography systems. *Radiat Prot Dosim* 2008;129:271-5.
 - Tapiovaara MJ. Review of relationships between physical measurements and user evaluation of image quality. *Radiat Prot Dosim* 2008;129:244-8.
 - Guibelalde E, Vano E. Design criteria for and evaluation of phantoms employed in conventional radiography. *Radiat Prot Dosim* 1993;49:39-46.
 - Chotas HG, Floyd CE, Johnson GA, Ravin CE. Quality control phantom for digital chest radiography. *Radiology* 1997;202:111-6.
 - Mah E, Samei E, Peck DJ. Evaluation of a quality control phantom for digital chest radiography. *J Appl Clin Med Phys* 2001;2:90-101.
 - International Commission on Radiation Units and Measurements (ICRU). Phantoms and computational models in therapy, diagnosis and protection. ICRU Report 48, ICRU; 1992.
 - International Commission on Radiation Units and Measurements (ICRU). Tissue substitutes in radiation dosimetry and measurements. ICRU Report 44, ICRU; 1989.
 - Martin CJ. The importance of radiation quality for optimization in radiology. *Biomedical Imaging and Interventional Journal*; 2007. Available from: <http://www.bijj.org/2007/2/e38>, doi:10.2349/bijj.3.2.e38 [Last accessed on 2010 Apr 30].
 - Fenner JW, Morrison GD, Kerry J, West N. A practical demonstration of improved technique factors in paediatric fluoroscopy. *Br J Radiol* 2002;75:596-602.
 - Doyle P, Martin CJ, Gentle D. Application of contrast-to-noise ratio in optimizing beam quality for digital chest radiography: Comparison of experimental measurements and theoretical simulations. *Phys Med Biol* 2006;51:2953-70.
 - Llorca AL, Guibelalde E, Vano E, Ruiz MJ. Analysis of image quality parameters using a combination of ANSI type phantom and the Leeds TOR (CDR) test object in simulations of simple examinations.

- Radiat Prot Dosim 1993;49:47-9.
15. Samei E, Dobbins JT 3rd, Lo JY, Tornai MP. A Framework for optimising the radiographic technique in digital x-ray imaging. *Radiat Prot Dosim* 2005;114:220-9.
 16. Rehani MM. Protection of patients in general radiography. International Atomic Energy Agency. Proceedings of the International Conference 26-30 March 2001, Malaga. Vienna, Austria: International Atomic Energy Agency; 2001. p. 169-80.
 17. Available from: http://www.leadstestobjects.com/modules/products/product_setup/file_library/TO%20%20poster.pdf [Last accessed on 2009 July 20].
 18. Rasband WS, Image J. U. S. National Institutes of Health. Bethesda, Maryland, USA. Available from: <http://rsb.info.nih.gov/ij/>, 1997-2006.
 19. Abramoff MD, Magelhaes PJ, Ram SJ. Image Processing with Image J. *Biophotonics Int* 2004;11:36-42.
 20. Van Engen R, Young K, Bosmans H, Thijsen M. The European protocol for the quality control of physical and technical aspects of mammography screening Part B Digital mammography. In the 4th ed. of the European Guidelines for Breast cancer screening, European Commission; 2005.
 21. Muhogora WE, Devetti A, Padovani R, Msaki P, Bonutti F. Application of European protocol in the evaluation of contrast-to-noise ratio and mean glandular dose for two digital mammography systems. *Radiat Prot Dosim* 2008;129:231-6.
 22. Marshall NW. An examination of automatic exposure control regimes for two digital radiography systems. *Phys Med Biol* 2009;54:4645-70.
 23. Bosmans H, Carton AK, Rogge F, Zanca F, Jacobs J, Van Ongeal C, *et al.* Image quality measurements and metrics in full field digital mammography: An overview. *Radiat Prot Dosim* 2005;117:120-30.
 24. Tucker DM, Rezendes PS. The relationship between pixel value and beam quality in photostimulable phosphor imaging. *Med Phys* 1997;24:887-93.
 25. Yaffe MJ, Rowlands JA. X-ray detectors for digital radiography. *Phys Med Biol* 1997;42:1-39.
 26. Sandborg M, Tingberg A, Ullman G, Dance DR. Comparison of clinical and physical measures of image quality in chest and pelvis computed radiography at different tube voltages. *Med Phys* 2006;33:4169-75.
 27. Honey ID, Mackenzie A, Evans DS. Investigation of optimum energies for chest imaging using film-screen and computed radiography. *Br J Radiol* 2005;78:422-7.
 28. McEntee M, Frawley H, Brenna PC. A comparison of low contrast performance for amorphous Silicon/Caesium iodide direct radiography with a computed radiography. A contrast detail phantom study. *Radiography* 2007;13:89-94.
 29. Venema HW, Den Heeten CJ. Digital radiography of the chest: Re-assessment of the high voltage technique? *Radiology* 2005;235(1):326-8.

Source of Support: Nil, **Conflict of Interest:** None declared.